

Design and optimization of solar parabolic trough collector with evacuated absorber by grey relational analysis

S. Arunkumar* and **K. Ramesh**

Department of Mechanical Engineering, Government College of Technology, Coimbatore 641 013, India

Solar energy that contains bright heat and light from the sun is often controlled using modern technology such as photovoltaic, solar heating, artificial photosynthesis, solar architecture and solar thermal electricity. This study concerned with an experimental analysis of solar parabolic trough collector. The sunlight is reflected from the parabolic trough surface and focused on the evacuated absorber tube. The trough is usually aligned to the N-S axis and can be rotated normally according to the sun position from east to west. We have studied the potential of a solar thermal system for hot-water generation. The parabolic trough concentrator was made of galvanized sheet metal on which solar reflective films were pasted. The heat transfer fluid, viz. water runs through the absorber tube and absorbs concentrated heat energy. It has been designed with principal focus 0.1 m from the vertex so that the receiver heat loss is minimized. Data were collected on water inlet temperature, outlet temperature of the heat transfer fluid, solar radiation and water flow rate (days) during March to May 2019 at Coimbatore, Tamil Nadu, India. Also, the processing parameters were optimized because they are the key factors affecting the performance of the solar collector. Grey relational analysis was used to solve the optimization. Through confirmatory experiments, the input variables such as time, angle of tracking and solar radiation, as well as output variables such as inlet temperature, outlet temperature and efficiency were obtained, and the optimal conditions were verified. A suitable choice of input parameters such as tracking angle of 120° provides a high efficiency rate at 2 pm for March, April and May.

Keywords: Evacuated absorber, grey relational analysis, parabolic trough collector, performance analysis, solar energy.

SOLAR energy is sustainable since it cannot be depleted in time applicable to the human race. The solar parabolic trough collector (PTC) or cylindrical parabolic collector employs linear imaging concentration. The performance of a PTC in the utilization of solar energy has been

studied earlier using the finite element method (FEM) method¹. Montes *et al.*² provided the results of designing a PTC and its applications in a solar thermal system for heat production. Gao *et al.*³ designed a novel, selective solar absorber coating of Al₂O₃ on a stainless steel substrate³. An experimental analysis was done using the absorber tube with internal hinged blades for the solar PTC. An average efficiency of 69.33% was noted compared to 60.82% for commercial absorber tubes⁴. The results of collector's structures mounted and the results were compared with computational and experimental data⁵. Analysis revealed thermal efficiency up to 60% (ref. 6). The pertinent applications of solar thermal systems have been reviewed⁷. A dynamic mathematical model was established and verified based on the photothermal conversion process of the PTC⁸. Materials, heat transfer characteristics and manufacturing challenges of the solar thermal collector were identified⁹. Javadi *et al.*¹⁰ proposed that the low-temperature solar collectors use water as the heat transfer fluid. Solar industrial process heating is considered as one of the clean and renewable energy options in several countries. It was proposed that a significant share of final energy consumption is in the industrial sectors¹¹. Concentrating solar power (CSP) technology is grooving up with exclusive devices because of high thermal performance was proposed¹². Reddy and Kumar¹³ presented mathematical techniques and simulation used in the design of parabolic trough solar systems along with a review on the applications. Kumaresan *et al.*¹⁴, evaluated the performance parameters of the PTC, such as useful heat gain, and thermal efficiency of individual/overall components of the system using therminol 55 heat transfer fluid. The fabrication and assembling method of a solar collector, newly evolved tools were proposed¹⁵. Fabrication and performance of the solar PTC with and without coatings on the receiver tube have been presented by Sagade *et al.*¹⁶. This study attempted to optimize the operational parameters and the optimal parameters of the solar collector¹⁷. The optimum solar parabolic trough parameters of temperature, optical efficiency and thermal efficiency were analysed using grey relational analysis¹⁷. The result shows the evacuated absorber is most efficient for the collector's overall performance¹⁸.

*For correspondence. (e-mail: arunkumarresearch2018@gmail.com)

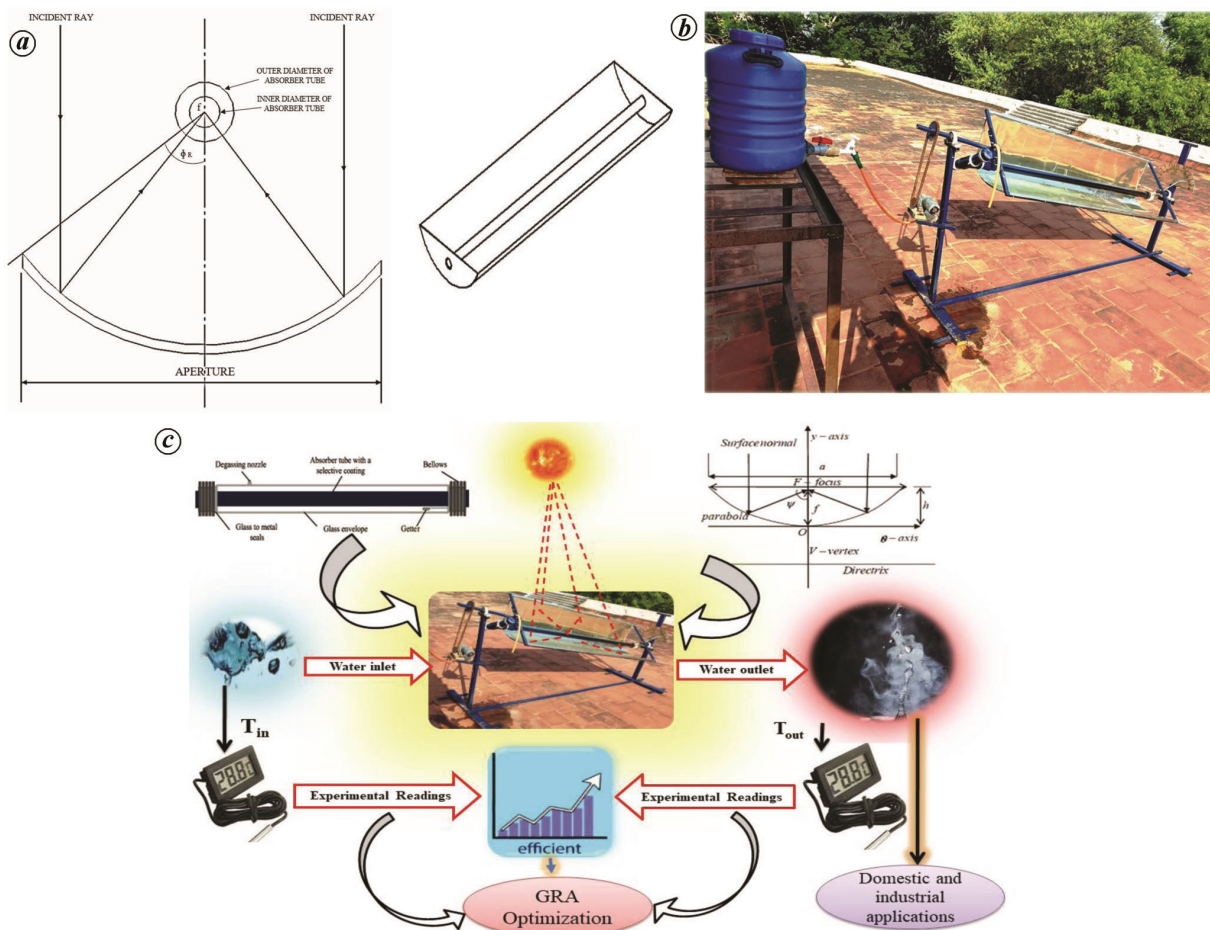


Figure 1. *a*, 2D geometry of the solar parabolic trough collector (PTC). *b*, Performance test set-up of the solar PTC. *c*, Experimental procedure and measurements.

Table 1. Design specifications of the parabolic trough collector

Components	Dimensions (mm)
Parabolic concentrator	Length – 1800 Aperture – 540 Focal length – 100
Evacuate absorber tube	Inner diameter – 47 Outer diameter – 58 Length – 1800
Support stand	Height due south – 1000 Height due north – 600 Distance between the two stands – 2200

Geometry of parabolic trough solar collector

Parabolic troughs have a focal line, which consists of the focal points of the parabolic cross-sections. As shown in Figure 1 *a*, radiation that enters in a plane parallel to the optical plane is reflected such that it passes through the focal line. The evacuated tube was used as the absorber due to no heat loss in the evacuated tube. Table 1 shows the design specifications of the solar PTC. The focal

length and rim angle of the PTC can be defined as follows¹⁹:

$$f = Y_s^2/4h, \quad (1)$$

$$\tan \varphi_R = 8(f/Y_s)/(16(f/Y_s)^2 - 1), \quad (2)$$

where f is the focal length of parabolic trough, Y_s the half length of collector aperture, h the height and φ is the rim angle.

Experimental study

Description of the performance test set-up

The essential components of the PTC such as concentrator and absorber tube were designed and fabricated with the above-mentioned specifications (Table 1). Figure 1 *b* shows the complete experimental set-up. The entire test set-up was positioned on the terrace of the Manufacturing Engineering building, Government College of Technology-Coimbatore, Tamil Nadu, India. A mechanical chain-drive

Table 2. Experimental particulars of March 2019

Day	Trial no.	Time	Angle of tracking (°)	Inlet temperature (°C)	Outlet temperature (°C)	Solar radiation (W/m ²)	Efficiency (%)
1	1	10.00 am	60	29	43	620	29.95
	2	11.00 am	75	29	58	790	48.70
	3	12.00 pm	90	29	51	980	29.78
	4	01.00 pm	105	30	56	1086	31.76
	5	02.00 pm	120	30	68	916	55.03
	6	03.00 pm	135	31	54	637	47.90
2	7	10.00 am	60	30	39	580	20.58
	8	11.00 am	75	30	50	815	32.55
	9	12.00 pm	90	30	58	917	40.51
	10	01.00 pm	105	30	60	1001	39.76
	11	02.00 pm	120	31	65	904	49.89
	12	03.00 pm	135	31	52	640	43.53
3	13	10.00 am	60	29	39	642	20.66
	14	11.00 am	75	29	45	860	24.68
	15	12.00 pm	90	29	63	979	46.07
	16	01.00 pm	105	29	63	1099	41.04
	17	02.00 pm	120	30	68	929	54.26
	18	03.00 pm	135	30	55	663	50.02
4	19	10.00 am	60	29	41	720	22.11
	20	11.00 am	75	29	52	852	35.81
	21	12.00 pm	90	29	55	1053	32.75
	22	01.00 pm	105	29	62	986	44.40
	23	02.00 pm	120	29	70	1008	53.96
	24	03.00 pm	135	30	60	886	44.92

system was provided to alter the angle of the PTC. Water was used as the heat transfer fluid and was calculated inside the evacuated absorber tube at a flow rate of 11 litre/h using the principle of thermosiphon.

Experimental procedure

Performance analysis of the solar PTC was carried out during different days of March, April and May at relevant time intervals. Experiments were conducted with three different input parameters, viz. time, angle of tracking and solar radiation and two output parameters, viz. inlet and outlet temperature of the heat transfer fluid. Six trials were performed per day with different tracking angles for all of three months. Totally 24 trials were performed per month. A digital thermometer was used for measuring inlet and outlet temperature of the heat transfer fluid. Figure 1 c shows the experimental procedure and measurements.

Efficiency is the most significant feature to quantify the performance level of the collector. The useful heat gain and instantaneous efficiency can be determined as follows

$$Q_u = mC_p(T_{\text{out}} - T_{\text{in}}), \quad (3)$$

$$\eta = Q_u/I_b r_b WL. \quad (4)$$

where Q_u is the useful heat gain, m the mass flow rate of fluid, C_p the specific heat of fluid, T_{out} the outlet

temperature of fluid and T_{in} is the inlet temperature of fluid. $I_b r_b$ is the incident solar radiation, W the width of the parabolic trough and L is the length of absorber tube.

Tables 2–4 provide the particulars of input and output variables of the solar PTC with evacuated absorber tube. The outlet temperature of the heat transfer fluid was obtained at relevant time intervals on different days of March, April and May 2019 respectively, and the instantaneous efficiency of the collector was predicted based on the readings obtained.

Results and discussion

The solar PTC with absorber tube was heated under the solar radiation conditions of Coimbatore. The graphs (Figures 2–4) are premeditated between time, outlet temperature of fluid, efficiency and solar radiation. Graphs were plotted from experimental readings for 12 days during March to May 2019.

The outlet temperature of the heat transfer fluid was increased gradually in the morning and it reached the highest value at 2 pm on all days of March 2019 (Figure 2 a). The highest values of outlet temperature were 68°C (day 1), 65°C (day 2), 68°C (day 3) and 70°C (day 4). The efficiency of the collector increased with a gradual increase in solar radiation and it decreased to lower when the radiation decreased concerning time (Figure 2 b). The highest values were 55.03%, 49.89%, 54.26% and 53.96%, obtained at 2 pm on all days of March 2019. It was found

Table 3. Experimental particulars of April 2019

Day	Trial no.	Time	Angle of tracking (°)	Inlet temperature (°C)	Outlet temperature (°C)	Solar radiation (W/m ²)	Efficiency (%)
1	1	10.00 am	60	29	48	690	36.53
	2	11.00 am	75	29	55	875	39.42
	3	12.00 pm	90	30	60	966	41.20
	4	01.00 pm	105	30	71	1033	52.65
	5	02.00 pm	120	30	82	910	75.81
	6	03.00 pm	135	30	58	630	58.96
2	7	10.00 am	60	29	36	684	13.57
	8	11.00 am	75	29	48	798	31.58
	9	12.00 pm	90	29	55	929	37.13
	10	01.00 pm	105	30	70	958	55.39
	11	02.00 pm	120	30	75	910	65.60
	12	03.00 pm	135	30	59	664	57.94
3	13	10.00 am	60	30	36	720	11.05
	14	11.00 am	75	30	45	921	21.60
	15	12.00 pm	90	30	56	1008	34.22
	16	01.00 pm	105	31	60	1073	35.85
	17	02.00 pm	120	30	78	933	68.25
	18	03.00 pm	135	30	60	762	52.23
4	19	10.00 am	60	30	39	762	15.67
	20	11.00 am	75	30	51	897	31.06
	21	12.00 pm	90	30	52	1002	29.13
	22	01.00 pm	105	30	60	1073	37.09
	23	02.00 pm	120	31	70	933	55.45
	24	03.00 pm	135	30	48	729	32.75

Table 4. Experimental particulars of May 2019

Day	Trial no.	Time	Angle of tracking (°)	Inlet temperature (°C)	Outlet temperature (°C)	Solar radiation (W/m ²)	Efficiency (%)
1	1	10.00 am	60	29	42	769	22.42
	2	11.00 am	75	29	48	881	28.61
	3	12.00 pm	90	29	56	932	38.43
	4	01.00 pm	105	30	62	920	46.14
	5	02.00 pm	120	30	74	808	72.24
	6	03.00 pm	135	30	60	763	52.16
2	7	10.00 am	60	30	39	762	15.67
	8	11.00 am	75	30	48	848	28.16
	9	12.00 pm	90	30	54	861	36.98
	10	01.00 pm	105	30	53	838	36.41
	11	02.00 pm	120	31	62	772	53.27
	12	03.00 pm	135	31	54	658	46.37
3	13	10.00 am	60	29	44	701	28.38
	14	11.00 am	75	29	47	793	30.11
	15	12.00 pm	90	30	51	864	32.24
	16	01.00 pm	105	30	53	853	35.77
	17	02.00 pm	120	30	63	779	56.20
	18	03.00 pm	135	30	57	667	53.70
4	19	10.00 am	60	28	37	734	16.26
	20	11.00 am	75	28	49	833	33.44
	21	12.00 pm	90	29	53	881	36.14
	22	01.00 pm	105	29	57	849	43.75
	23	02.00 pm	120	29	51	763	38.25
	24	03.00 pm	135	29	47	663	36.02

that the maximum amount of radiation was measured at 1 pm on all days (1086, 1001, 1099 and 1053 W/m²) (Figure 2 c).

The outlet temperature of heat transfer fluid was increased during the morning and it reached the highest value at 2 pm on all days of April 2019 (Figure 3 a). The

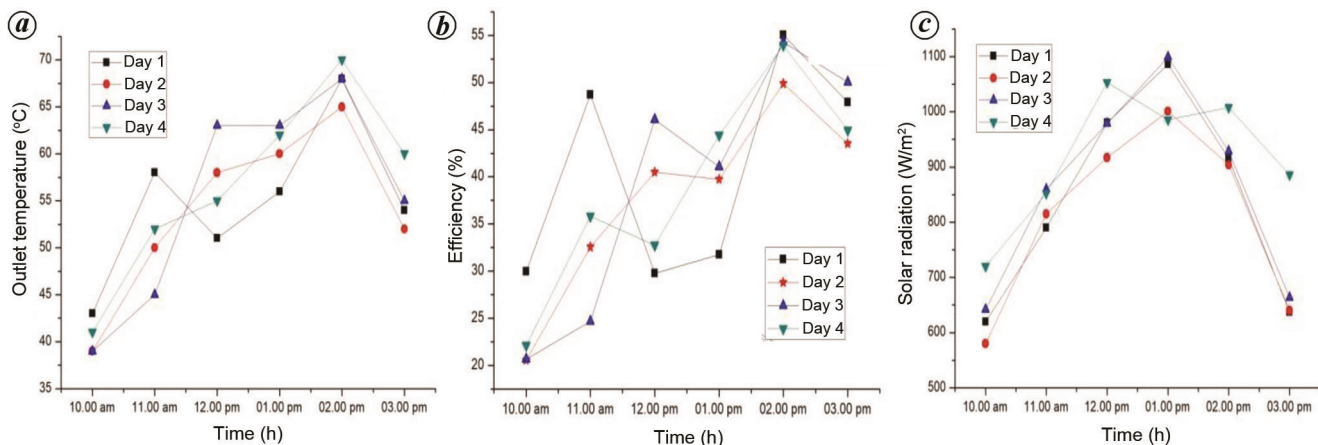


Figure 2. (a) Outlet temperature of heat transfer fluid (HTF); (b) Efficiency rate of PTC; (c) Measured solar radiation in March 2019.

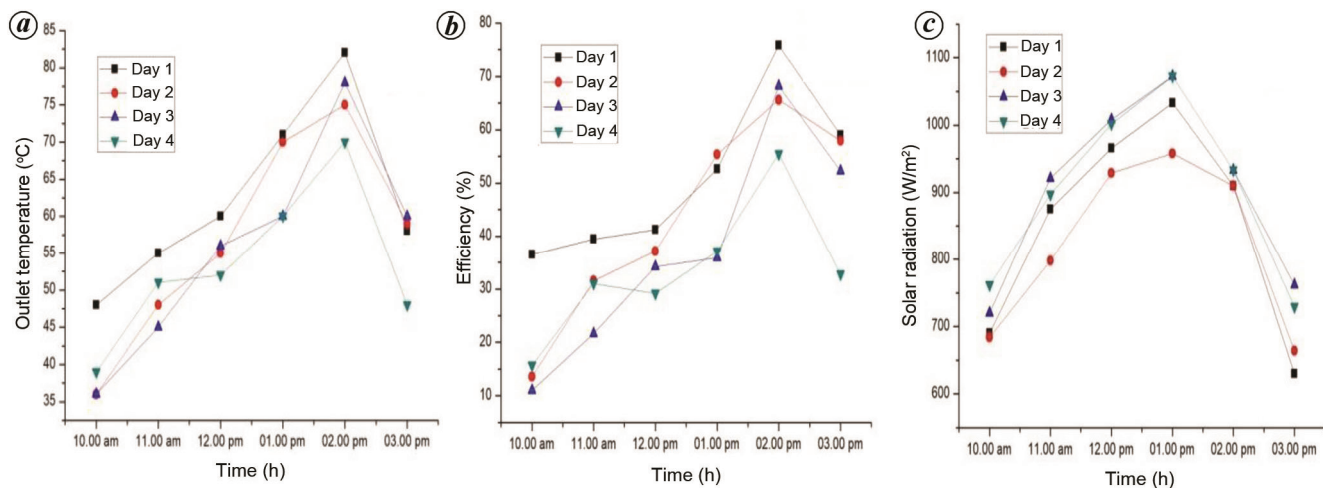


Figure 3. (a) Outlet temperature of HTF; (b) Efficiency rate of PTC; (c) Measured solar radiation in April 2019.

maximum values of outlet temperature were 82°C, 75°C, 78°C and 70°C. The efficiency of the PTC increased with a gradual increase in solar radiation (Figure 3 b). The maximum values were 75.81%, 65.60%, 68.25% and 55.45%, which were obtained at 2 pm on all days of April 2019. It was found that the maximum amount of radiation was measured at 1 pm on all days, 1033, 958, 1073 and 1073 W/m² (Figure 3 c).

The outlet temperature of the fluid was increased during the morning and it showed highest value at 2 pm on the first three days and 1 pm on the fourth day of May 2019 (Figure 4 a). The highest values of outlet temperature were 74°C, 62°C, 63°C and 57°C respectively. The maximum values of solar parabolic trough efficiency were 72.24%, 53.27%, 56.20% and 43.75%, which were obtained concerned to outlet temperature (Figure 4 b). It had been found that the maximum amount of radiation was measured at 12 noon on all days (932, 861, 864 and 881 W/m²) (Figure 4 c).

Figure 5 a shows the overall performance of the solar PTC with evacuated absorber tube. A comparison was

made between the months of March, April and May. The highest efficiency of the collector was found to be 75.81% on 1 April 2019 at 2 pm.

Grey relational analysis

Grey relational analysis is a technique to evaluate the relationship grade between factors based on the correspondence or variation between them. It is characterized by less data and multifactor analysis, where these two uniqueness can conquer the disadvantages of the statistical regression analysis. Performance and efficiency are important for both consumers and manufacturers. The objectives of the present study were maximizing the outlet temperature of the heat transfer fluid and the efficiency of the solar collector. The procedure of the grey relational analysis is as follows: (i) Experimental data were first normalized ranging from 0 to 1. (ii) Grey relational coefficient was estimated based on normalized experimental data. (iii) Overall grey relational grade (GRG) was obtained

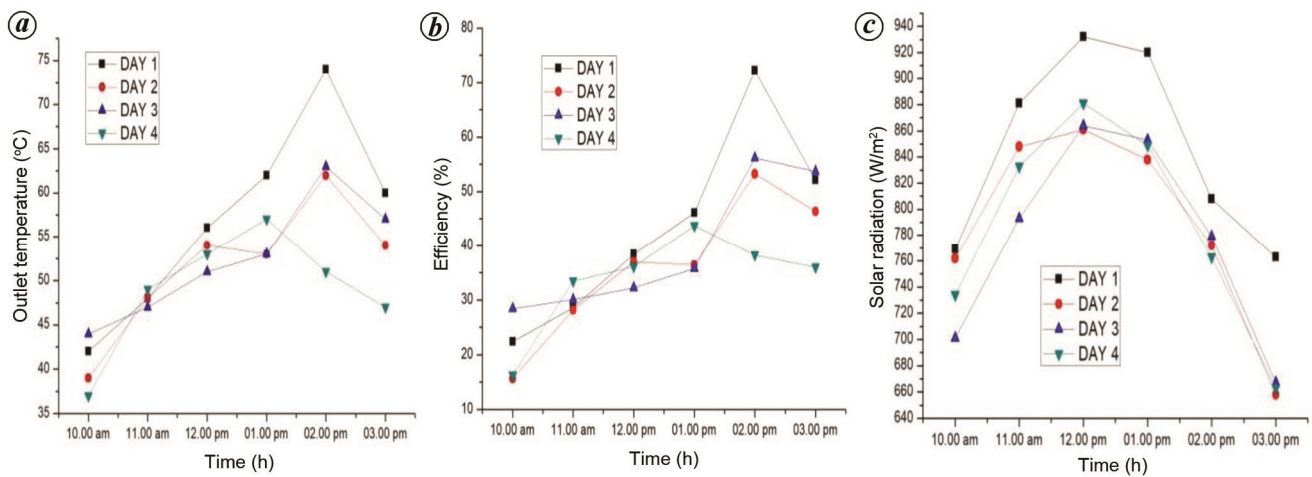


Figure 4. (a) Outlet temperature of HTF; (b) Efficiency rate of PTC; (c) Measured solar radiation in May 2019.

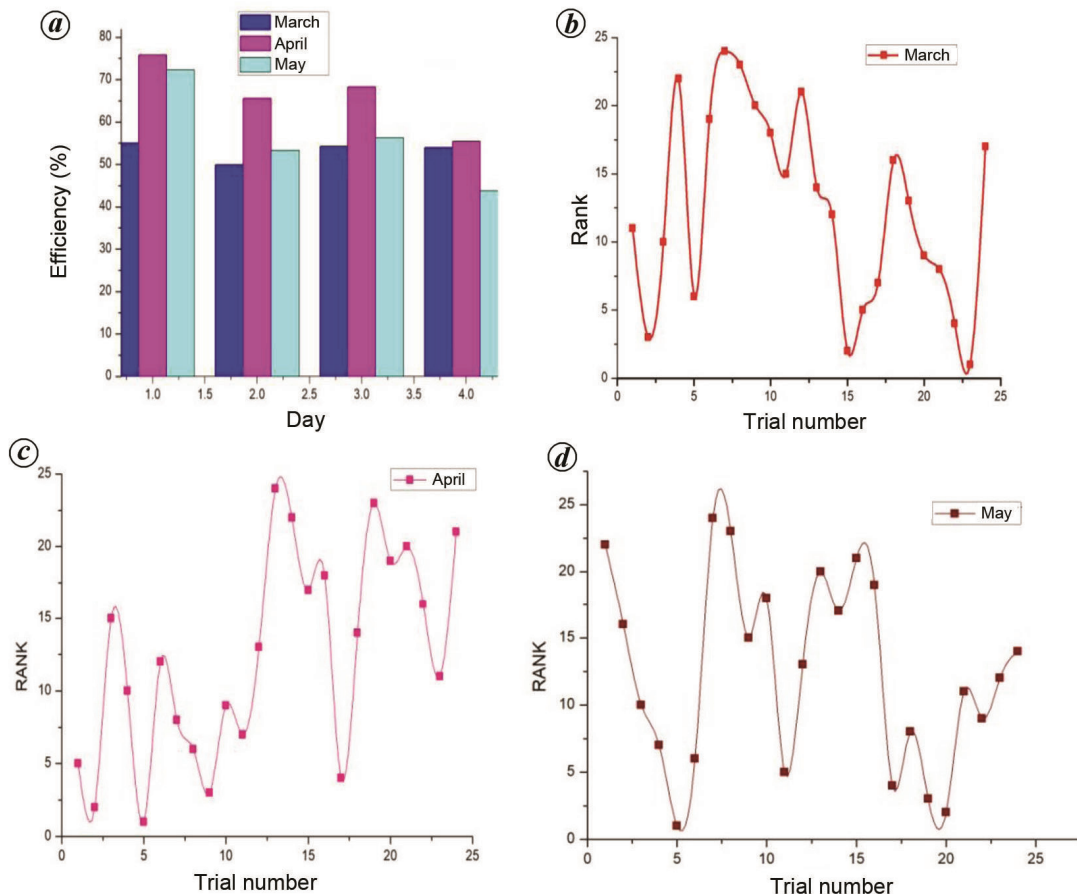


Figure 5. (a) Overall efficiency. Grey relational grade for (b) March 2019; (c) April 2019; (d) May 2019.

by averaging the grey relational coefficients of each chosen response.

Step 1: Normalization – In the case of ‘lower the better’ (in the result that the smaller the target value, the better

i.e. inlet temperature of heat transfer fluid), the original array can be normalized as follows

$$Y_i(a) = \frac{[\max(X_i(a)) - X_i(a)]}{[\max(X_i(a)) - \min(X_i(a))]}, \quad (5)$$

Table 5. Grey relational analysis for March 2019

Trial no.	Normalized data			Deviated data			Grey relational coefficient			Grey relational grade (GRG)	Rank
	T_{in} (°C)	T_{out} (°C)	η (%)	T_{in} (°C)	T_{out} (°C)	η (%)	T_{in} (°C)	T_{out} (°C)	η (%)		
1	1	0.1290	0.2719	0	0.8709	0.7280	1	0.3147	0.3546	0.5564	11
2	1	0.6129	0.8162	0	0.3870	0.1837	1	0.5081	0.6852	0.7311	3
3	1	0.3870	0.2670	0	0.6129	0.7329	1	0.3949	0.3530	0.5826	10
4	0.5	0.5483	0.3245	0.5	0.4516	0.6754	0.1666	0.4696	0.3719	0.3360	22
5	0.5	0.9354	1	0.5	0.0645	0	0.1666	0.8611	1	0.6759	6
6	0	0.4838	0.7930	1	0.5161	0.2069	0.0909	0.4366	0.6590	0.3955	19
7	0.5	0	0	0.5	1	1	0.1666	0.2857	0.2857	0.2460	24
8	0.5	0.3548	0.3474	0.5	0.6451	0.6525	0.1666	0.3827	0.3800	0.3098	23
9	0.5	0.6129	0.5785	0.5	0.3870	0.4214	0.1666	0.5081	0.4869	0.3872	20
10	0.5	0.6774	0.5567	0.5	0.3225	0.4432	0.1666	0.5535	0.4743	0.3981	18
11	0	0.8387	0.8507	1	0.1612	0.1492	0.0909	0.7126	0.7283	0.5106	15
12	0	0.4193	0.6661	1	0.5806	0.3338	0.0909	0.4078	0.5450	0.3479	21
13	1	0	0.0023	0	1	0.9976	1	0.2857	0.2861	0.5239	14
14	1	0.1935	0.1190	0	0.8064	0.8809	1	0.3315	0.3122	0.5479	12
15	1	0.7741	0.7399	0	0.2258	0.2600	1	0.6391	0.6059	0.7483	2
16	1	0.7741	0.5939	0	0.2258	0.4060	1	0.6391	0.4962	0.7117	5
17	0.5	0.9354	0.9776	0.5	0.0645	0.0223	0.1666	0.8611	0.9470	0.6582	7
18	0.5	0.5161	0.8545	0.5	0.4838	0.1454	0.1666	0.4525	0.7333	0.4508	16
19	1	0.0645	0.0444	0	0.9354	0.9555	1	0.2995	0.2950	0.5315	13
20	1	0.4193	0.4420	0	0.5806	0.5579	1	0.4078	0.4175	0.6084	9
21	1	0.5161	0.3532	0	0.4838	0.6467	1	0.4525	0.3821	0.6115	8
22	1	0.7419	0.6914	0	0.2580	0.3085	1	0.6078	0.5645	0.7241	4
23	1	1	0.9689	0	0	0.0310	1	1	0.9279	0.9759	1
24	0.5	0.6774	0.7065	0.5	0.3225	0.2934	0.1666	0.5535	0.5768	0.4323	17

In the case of ‘higher the better’ (in the result that the larger the target value, the better, i.e. outlet temperature of heat transfer fluid and efficiency), the original array can be normalized as follows

$$Y_i(a) = \frac{[X_i(a) - \min(X_i(a))]}{[\max(X_i(a)) - \min(X_i(a))]}, \quad (6)$$

where $Y_i(a)$ is the sequence after data pre-processing, $X_i(a)$ the actual sequence, $X_i(a) = 1$ the first value of the sequence, $\max(X_i(a))$ the largest value of $X_i(a)$ and $\min(X_i(a))$ is the smallest value of $X_i(a)$.

Step 2: Calculation of Grey relational coefficients – The grey relational coefficient ($\xi_i(a)$) can be calculated as follows

$$\xi_i(a) = \frac{[D_{min} + \xi D_{max}]}{[D_i(a) + \xi D_{max}]}, \quad (7)$$

where $D_i(a)$ is the deviation sequence (i.e. absolute value of the difference between $X_i(a)$ and $Y_i(a)$), D_{min} the smallest value of $D_i(a)$, D_{max} the largest value of $D_i(a)$ and ξ is the distinguishing coefficient.

Step 3: To determine GRG – GRG is the average value of grey relational coefficients and is defined as follows

$$\psi_i = 1/n \sum_{a=1}^n w_a \xi_i(a), \quad (8)$$

where w_a is the normalized weightage of factor a .

From the experiment, the input variables such as time, angle of tracking and solar radiation, and the output variables such as inlet temperature, outlet temperature and efficiency were obtained. The normalized data, deviated data, grey relational coefficients, GRG and rank of each experimental trial (March–May) were determined using eqs (5)–(8). Tables 5–7 show the results.

In this analysis, outlet temperature of the heat transfer fluid and efficiency of the PTC were assigned higher weightage than inlet temperature of the heat transfer fluid. The following values of weightage were assigned for different variables, viz. outlet temperature = 0.4, efficiency = 0.4 and inlet temperature = 0.2.

Table 5 shows that trial number 23 has GRG of 0.9759; thus, the parameter setting of trial number 23 is likely to be optimal. Table 6 shows that trial number 5 has GRG of 0.7222; thus, the parameter setting of trial number 5 is likely to be optimal. Table 7 shows that trial number 5 has GRG of 0.7101; thus, the parameter setting of trial number 23 is likely to be optimal. Figure 5 *b*, *c* and *d* shows the relationship between trial number and rank of performance level for March, April and May respectively. Table 8 shows the results of optimal conditions for input and output variables. By the application of grey relational analysis, the optimal parameters of the solar PTC were predicted rank-wise for all the three months.

Conclusion

This work focused on the design, experimental study and optimization of a solar PTC with evacuated absorber. The

Table 6. Grey relational analysis for April 2019

Trial no.	Normalized data			Deviated data			Grey relational coefficient			GRG	Rank
	T_{in} (°C)	T_{out} (°C)	η (%)	T_{in} (°C)	T_{out} (°C)	η (%)	T_{in} (°C)	T_{out} (°C)	η (%)		
1	1	0.2608	0.3934	0	0.7391	0.6065	1	0.3511	0.3973	0.58284	5
2	1	0.4130	0.4380	0	0.5869	0.5619	1	0.4052	0.4158	0.60704	2
3	0.5	0.5217	0.4655	0.5	0.4782	0.5344	0.1666	0.4554	0.4280	0.35005	15
4	0.5	0.7608	0.6423	0.5	0.2391	0.3576	0.1666	0.6258	0.5279	0.44016	10
5	0.5	1	1	0.5	0	0	0.1666	1	1	0.72222	1
6	0.5	0.4782	0.7398	0.5	0.5217	0.2601	0.1666	0.4339	0.6058	0.40217	12
7	1	0	0.0389	0	1	0.9610	1	0.2857	0.2938	0.52653	8
8	1	0.2608	0.3170	0	0.7391	0.6829	1	0.3511	0.3693	0.57349	6
9	1	0.4130	0.4027	0	0.5869	0.5972	1	0.4052	0.4010	0.60212	3
10	0.5	0.7391	0.6846	0.5	0.2608	0.3153	0.1666	0.6052	0.5591	0.44370	9
11	0.5	0.8478	0.8423	0.5	0.1521	0.1576	0.1666	0.7244	0.7172	0.53612	7
12	0.5	0.5	0.7240	0.5	0.5	0.2759	0.1666	0.4444	0.5917	0.40095	13
13	0.5	0	0	0.5	1	1	0.1666	0.2857	0.2857	0.24603	24
14	0.5	0.1956	0.1629	0.5	0.8043	0.8370	0.1666	0.3321	0.3233	0.27404	22
15	0.5	0.4347	0.3577	0.5	0.5652	0.6422	0.1666	0.4144	0.3837	0.32162	17
16	0	0.5217	0.3829	1	0.4782	0.6170	0.0909	0.4554	0.3932	0.31321	18
17	0.5	0.9130	0.8832	0.5	0.0869	0.1167	0.1666	0.8214	0.7740	0.58739	4
18	0.5	0.5217	0.6358	0.5	0.4782	0.3641	0.1666	0.4554	0.5234	0.38186	14
19	0.5	0.0652	0.0713	0.5	0.9347	0.9286	0.1666	0.2996	0.3010	0.25579	23
20	0.5	0.3260	0.3089	0	0.6739	0.6910	0.1666	0.3724	0.3666	0.30192	19
21	0.5	0.3478	0.2791	0.5	0.6521	0.7208	0.1666	0.3801	0.3568	0.30123	20
22	0.5	0.5217	0.4021	0.5	0.4782	0.5979	0.1666	0.4554	0.4008	0.34098	16
23	0	0.7391	0.6856	1	0.2608	0.3143	0.0909	0.6052	0.5599	0.41869	11
24	0.5	0.2608	0.3350	0.5	0.7391	0.6649	0.1666	0.3511	0.3756	0.29780	21

Table 7. Grey relational analysis for May 2019

Trial no.	Normalized data			Deviated data			Grey relational coefficient			GRG	Rank
	T_{in} (°C)	T_{out} (°C)	η (%)	T_{in} (°C)	T_{out} (°C)	η (%)	T_{in} (°C)	T_{out} (°C)	η (%)		
1	0.66	0.1351	0.1193	0.33	0.8648	0.8806	0.2307	0.3162	0.3123	0.28644	22
2	0.66	0.2972	0.2287	0.33	0.7027	0.7712	0.2307	0.3627	0.3415	0.31167	16
3	0.66	0.5135	0.4023	0.33	0.4864	0.5976	0.2307	0.4512	0.4009	0.36097	10
4	0.33	0.6756	0.5386	0.66	0.3243	0.4613	0.1304	0.5522	0.4643	0.38234	7
5	0.33	1	1	0.66	0	0	0.1304	1	1	0.71014	1
6	0.33	0.6216	0.6450	0.66	0.3783	0.3549	0.1304	0.5138	0.5298	0.39138	6
7	0.33	0.0540	0	0.66	0.9459	1	0.1304	0.2971	0.2857	0.23777	24
8	0.33	0.2972	0.2207	0.66	0.7027	0.7792	0.1304	0.3627	0.3392	0.27746	23
9	0.33	0.4594	0.3767	0.66	0.5405	0.6232	0.1304	0.4252	0.3908	0.31553	15
10	0.33	0.4324	0.3666	0.66	0.5675	0.6333	0.1304	0.4134	0.3870	0.31030	18
11	0	0.6756	0.6646	1	0.3243	0.3353	0.0909	0.5522	0.5439	0.39570	5
12	0	0.4594	0.5426	1	0.5405	0.4573	0.0909	0.4252	0.4665	0.32759	13
13	0.66	0.1891	0.2246	0.33	0.8108	0.7753	0.2307	0.3303	0.3403	0.30048	20
14	0.66	0.2702	0.2552	0.33	0.7297	0.7447	0.2307	0.3540	0.3494	0.31142	17
15	0.33	0.3783	0.2929	0.66	0.6216	0.7070	0.1304	0.3915	0.3613	0.29442	21
16	0.33	0.4324	0.3553	0.66	0.5675	0.6446	0.1304	0.4134	0.3828	0.30891	19
17	0.33	0.7027	0.7164	0.66	0.2972	0.2835	0.1304	0.5736	0.5851	0.42975	4
18	0.33	0.5405	0.6722	0.66	0.4594	0.3277	0.1304	0.4654	0.5496	0.38183	8
19	1	0	0.0104	0	1	0.9895	1	0.2857	0.2878	0.52452	3
20	1	0.3243	0.3141	0	0.6756	0.6858	1	0.3718	0.3683	0.58007	2
21	0.66	0.4324	0.3618	0.33	0.5675	0.6381	0.2307	0.4134	0.3853	0.34316	11
22	0.66	0.5405	0.4963	0.33	0.4594	0.5036	0.2307	0.4654	0.4426	0.37961	9
23	0.66	0.3783	0.3991	0.33	0.6216	0.6008	0.2307	0.3915	0.3996	0.34065	12
24	0.66	0.2702	0.3597	0.33	0.7297	0.6402	0.2307	0.3540	0.3845	0.32311	14

study was done during March–May 2019. The highest efficiency of 75.81% on 1 April 2019 at 2 pm was obtained for solar radiation of 910 W/m² and efficiency of 72.24% on 1 May 2019 at 2 pm was obtained for solar radiation of 808 W/m². For optimization, grey relational

analysis was applied with various parameters for predicting the time, angle of tracking and the required radiation. The responses were taken as temperature and thermal efficiency in this study. These responses should be maximized. The weightages used in the grey relational analysis were also

Table 8. Results of grey relational analysis optimal level

Optimal conditions	Time (h)	March			April			May		
		R1	R2	R3	R1	R2	R3	R1	R2	R3
Input variables	Angle of tracking (°)	120	90	75	120	75	90	120	75	60
	Solar radiation (W/m ²)	1008	979	790	910	875	929	808	833	734
Output variables	Inlet temperature (°C)	29	29	29	30	29	29	30	28	28
	Outlet temperature (°C)	70	63	58	82	55	55	74	49	37
	Efficiency (%)	53.9	46	48.7	75.8	39.4	37.13	72.2	33.4	16.2

varied. The optimal performance of the solar PTC for maximum outlet temperature of 82°C and efficiency of 75.8% was observed at angle of tracking 120° and solar radiation 910 W/m² at 2 pm (April 2019). Similarly, outlet temperature of 74°C and efficiency of 72.24% were obtained at angle of tracking 120° and solar radiation 808 W/m² at 2 pm (May 2019). Finally, the highest outlet temperature rate of the heat transfer fluid, efficiency rate of the solar PTC were found. Similar optimal conditions were also predicted and validated by grey relational analysis.

1. Wang, Y., Liu, Q., Lei, J. and Jin, H., Performance analysis of a parabolic trough solar collector with non-uniform solar flux conditions. *Int. J. Heat Mass Transfer*, 2015, **82**, 236–249.
2. Montes, I. E. P., Benitez, A. M., Chavez, O. M. and Herrera, A. E. L., Design and construction of a parabolic trough solar collector for process heat production. *Energy Procedia*, 2014, **57**, 2149–2158.
3. Gao, X.-H., Guo, Z.-M., Geng, Q.-F., Ma, P.-J., Wang, A.-Q. and Liu, G., Microstructure, chromaticity and thermal stability of SS/TiC-WC/Al₂O₃ spectrally selective solar absorbers. *Sol. Energy Mater. Sol. Cells*, 2017, **164**, 63–69.
4. Kalidasan, B., Shankar, R. and Srinivas, T., Absorber tube with internal hinged blades for solar parabolic trough collector. *Energy Procedia*, 2016, **90**, 463–469.
5. Tagle, P. D., Agraz, A. and Rivera, C. I., Study of applications of parabolic trough solar collector technology in Mexican industry. *Energy Procedia*, 2016, **91**, 661–667.
6. Agraz, A., Metodología para la caracterización optimización de un concentrador solar parabólico lineal monterrey. Master's thesis, Engineering Science School, 2012.
7. Jebasingh, V. K. and Joselin Herbert, G. M., A review of solar parabolic trough collector. *Renew. Sustain. Energy Rev.*, 2016, **54**, 1085–1091.
8. Luo, N., Yu, G., Hou, H. J. and Yang, Y. P., Dynamic modelling and simulation of parabolic trough solar system. *Energy Procedia*, 2015, **69**, 1344–1348.
9. Rashidi, S., Esfahani, J. A. and Rashidi, A., A review on the applications of porous materials in solar energy systems. *Renew. Sustain. Energy Rev.*, 2017, **73**, 1198–1210.
10. Javadi, F., Saidur, A. R. and Kamalisarvestani, M., Investigating performance improvement of solar collectors by using nanofluids. *Renew. Sustain. Energy Rev.*, 2013, **28**, 232–245.
11. Suman, S., Khan, M. and Pathak, M., Performance enhancement of solar collectors – a review. *Renew. Sustain. Energy Rev.*, 2015, **49**, 192–210.
12. Ummadisingu, A. and Soni, M. S., Concentrating solar power-technology potential and policy in India. *Renew. Sustain. Energy Rev.*, 2011, **15**, 5169–5175.
13. Reddy, K. S. and Kumar, K. R., Energy for sustainable development solar collector field design and viability analysis of stand-alone parabolic trough power plants for Indian conditions. *Energy – Sustain. Div.*, 2012, **16**, 456–470.
14. Kumaresan, G., Sridhar, R. and Velraj, R., Performance studies of a solar parabolic trough collector with a thermal energy storage system. *Energy*, 2012, **47**, 395–402.
15. Schweitzer, A., Schiel, W., Birkle, M., Nava, P., Riffelmann, K. and Wohlfahrt, A., Fabrication, erection and commissioning of the world's largest parabolic trough collector. *Energy Procedia*, 2014, **49**, 1848–1857.
16. Sagade, A., Aher, S. and Shinde, N., Performance evaluation of low-cost FRP parabolic trough reflector with mild steel receiver. *Int. J. Energy Environ. Eng.*, 2013, **4**, 5–11.
17. Jeffrey Kuo, C.-F., Su, T.-L., Jhang, P.-R., Huang, C.-Y. and Chiu, C.-H., Using the Taguchi method and grey relational analysis to optimize the flat-plate collector process with multiple quality characteristics in solar energy collector manufacturing. *Energy*, 2011, **36**, 3554–3562.
18. Mohana Reddy, P., Venkataramaiah, P. and Sairam, P., Optimization of process parameters of a solar parabolic trough in winter using grey–Taguchi approach. *Int. J. Res. Appl.*, 2012, **2**, 816–821.
19. Sukhatme, S. P. and Nayak, J. K., *Solar Energy*, McGraw Hill Education, India, 2017, 4th edn.

Received 12 January 2020; revised accepted 27 December 2021

doi: 10.18520/cs/v122/i4/410-418